



# Rate enhancement in collisions of sulfuric acid molecules due to long-range intermolecular forces

Roope Halonen<sup>1</sup>, Evgeni Zapadinsky<sup>1</sup>, Theo Kurtén<sup>2</sup>, Hanna Vehkamäki<sup>1</sup>, and Bernhard Reischl<sup>1</sup>

<sup>1</sup>Institute for Atmospheric and Earth System Research / Physics, Faculty of Science, University of Helsinki, P.O. Box 64, FI-00014, Finland

<sup>2</sup>Institute for Atmospheric and Earth System Research / Chemistry, Faculty of Science, University of Helsinki, P.O. Box 55, FI-00014, Finland

**Correspondence:** Roope Halonen (roope.halonen@helsinki.fi)

**Abstract.** Collisions of molecules and clusters play a key role in determining the rate of atmospheric new particle formation and growth. Traditionally the statistics of these collisions are taken from kinetic gas theory assuming spherical non-interacting particles, which may significantly underestimate the collision coefficients for most atmospherically relevant molecules. Such systematic errors in predicted new particle formation rates will also affect large-scale climate models. We have studied the statistics of collisions of sulfuric acid molecules in vacuum by atomistic molecular dynamics simulations. We have found that the effective collision cross section of the H<sub>2</sub>SO<sub>4</sub> molecule, as described by an OPLS-All Atom force field, is significantly larger than the hard-sphere diameter assigned to the molecule based on the liquid density of sulfuric acid. As a consequence, the actual collision coefficient is enhanced by a factor 2.2, compared to kinetic gas theory. This enhancement factor obtained from atomistic simulation is consistent with the discrepancy observed between experimental formation rates of clusters containing sulfuric acid and calculated formation rates using hard sphere kinetics. We find reasonable agreement with an enhancement factor calculated from the Langevin model of capture, fitted to the attractive part of the atomistic intermolecular potential of mean force.

## 1 Introduction

New particle formation from condensable vapours gives an important contribution to the composition of aerosols in the atmosphere which affects air quality as well as the Earth's climate. The positive and negative contributions of atmospheric aerosols to the planet's radiative balance are still not fully understood, and currently constitute one of the largest uncertainties in climate modelling. The earliest stage of new particle formation involves collisions of individual molecules leading to the appearance of a new molecular complex. In many theoretical approaches, the statistics of such collisions are simply taken from kinetic gas theory, i.e. the molecules are considered to be non-interacting hard spheres, and a collision occurs when the impact parameter is smaller than the sum of the hard spheres' radii. The hard sphere collision cross section is independent of the relative velocity of the colliding bodies, and the collision rate coefficient for hard spheres of identical radii is customarily expressed as

$$\beta_{\text{HS}} = \sqrt{\frac{8k_{\text{B}}T}{\pi\mu}} \pi(2R)^2, \quad (1)$$



where  $k_B$  is Boltzmann's constant,  $T$  is the temperature,  $\mu$  is the reduced mass and  $R$  is the radius of the spheres.

It is well known that acid-base clusters, and in particular clusters containing sulfuric acid and ammonia, or amines, are very relevant in nucleation and growth of particles that can serve as cloud condensation nuclei (Almeida et al., 2013). Such molecules, however, are not necessarily spherical and despite being charge neutral, exhibit long-ranged attraction due to interactions between permanent dipoles, permanent and induced dipoles, or induced dipoles (Israelachvili, 2011). Therefore, it is reasonable to expect that particle growth rates or cluster size distributions predicted using collision coefficients from kinetic gas theory will have a systematic error, which needs to be accounted for. In fact, it has recently been found that collision coefficients obtained in this way had to be scaled by a factor 2.3–2.7 to predict kinetically limited nucleation rates in agreement with experiment, for a system containing sulfuric acid, dimethylamine and water (Kürten et al., 2014; Lehtipalo et al., 2016; Kürten et al., 2018).

The effect of long-range interactions between neutral polar molecules on the capture rate constant has been studied by classical trajectory integration (Maergoiz et al., 1996c). The interaction potential between the colliding parties has been approximated by two terms: First, an anisotropic interaction between permanent dipoles, proportional to  $r^{-3}$ , where  $r$  is the distance between the centres of mass of the molecules. Second, an isotropic term due to the interaction between permanent dipole and induce dipole, and the interaction between induced dipoles, proportional to  $r^{-6}$ . However, such an approximation is inaccurate when the distance between the colliding particles is comparable to their size. Rate coefficients for ion-molecule capture processes have also been studied theoretically in both classic and quantum regime (Moran and Hamill, 1963; Su and Bowers, 1973; Su et al., 1978; Chesnavich et al., 1980; Clary, 1985; Troe, 1987) or by using trajectory calculations (Dugan Jr. and Magee, 1967; Chesnavich et al., 1980; Su and Chesnavich, 1982; Maergoiz et al., 1996a, b). Atomistic simulations have been used to study collisions of Lennard-Jones clusters and atmospherically relevant molecules, but these studies did not analyze or report thermal collision rate coefficients (Napari et al., 2004; Loukonen et al., 2014). The influence of Van der Waals forces on the collision rate has also been considered in Brownian coagulation models of ultra-fine aerosol particles (Marlow, 1980; Sceats, 1986, 1989).

In the present work, we use atomistic molecular dynamics simulations to study the statistics of collisions between sulfuric acid molecules in vacuum, determine the collision rate coefficient and calculate the enhancement factor over kinetic gas theory. We are here focusing on “reactive” collisions, defined by the formation of one or more hydrogen bonds between the molecules. Detailed modelling of e.g. proton transfer processes related to hydrogen bond formation in such reactive collisions would require first principle simulations (Loukonen et al., 2014), however the need to simulate a large number of individual trajectories to cover a representative range of impact parameters and relative velocities makes this impossible. In the present study we are modelling the collision rate enhancement due to long-range interactions, which can be decently described by empirical force fields.

In section 2 we discuss technical matters of the choice of force field and the simulation setup and give a brief overview of the theoretical background for collisions of atmospheric particles. In section 3, simulation results are presented, discussed within the theoretical framework and compared to analytical and experimental results.



## 2 Simulation details and theoretical models

### 2.1 Force field benchmark

We have considered two force fields to describe the sulfuric acid molecules in the present study. The first choice was the force field by Ding et al. (2003), fitted specifically to reproduce DFT structures and energies of small clusters of sulfuric acid, bisulfate and water, in vacuum. The second choice was the force field by Loukonen et al. (2010), who had fitted interaction parameters for sulfuric acid, bisulfate and dimethylammonium according to the OPLS-All Atom procedure (Jorgensen et al., 1996). Both force fields are fitted to reproduce the  $C_2$  geometry of the isolated  $H_2SO_4$  molecule in vacuum, and the atoms' partial charges create dipole moments of 3.52 and 3.07 Debye, for Ding et al. and Loukonen et al., respectively, in agreement with experiments (2.7–3.0 Debye) and ab initio calculations (2.7–3.5 Debye) (Sedo et al., 2008). While in the OPLS force field intramolecular degrees of freedom are described by harmonic bonds and angles as well as dihedrals, the geometry of the molecule in the force field by Ding et al. is constrained using additional intramolecular harmonic potentials between non-bonded atoms.

To validate the force fields, we compare the structures and energies of four stable configurations of the sulfuric acid dimer illustrated in Fig. 1(a–d) to ab initio structures and energies at the RI-MP2/CBS//6-31+G\* level of theory calculated by Temelso et al. (2012). The results of the benchmark are summarised in Tab. 1. The force field by Ding et al. correctly predicts the lowest energy for dimer structure “a”, and the relative energy differences  $\Delta\Delta E$  between optimised structures are closer to those obtained in the ab initio calculation than for the OPLS force field, which assigns the lowest energy to structure “d”, which is the highest energy structure in the ab initio calculation. The geometries of the structures agree well with the ab initio result for both force fields, with the OPLS force field reproducing the ab initio hydrogen bond lengths slightly better than the force field by Ding et al. The binding energies at  $T = 0$  K are slightly lower for the force fields (–0.64 and –0.67 eV for OPLS, and Ding et al., respectively) compared to the ab initio value of –0.72 eV. Overall, the force field by Ding et al. performs slightly better in terms of energetics.

However, the vibrational spectra, calculated from the Fourier transform of the velocity autocorrelation functions of an isolated  $H_2SO_4$  molecule in vacuum, exhibit strong differences: while the force field by Loukonen et al. is able to reproduce the experimental and ab initio spectra very well (Hintze et al., 2003; Chackalackal and Stafford, 1966; Miller et al., 2005), the force field by Ding et al. is not, as shown in Fig. 2. Intramolecular vibrations are relevant in the context of molecular collisions, e.g. when studying energy transfer between different internal degrees of freedom during, and after the collision. Also, the OPLS-All Atom procedure allows for transferable potentials, as opposed to the Ding et al. force field which cannot easily be extended to other chemical compounds in future studies. For these two reasons, we decided to use the OPLS force field by Loukonen et al. for the collision simulations.

### 2.2 Potential of mean force of two sulfuric acid molecules

We first calculated the binding free energy of two sulfuric acid molecules in vacuum as described by the force fields of Loukonen et al. and Ding et al. The potential of mean force (PMF) as a function of the sulfur–sulfur distance was calculated

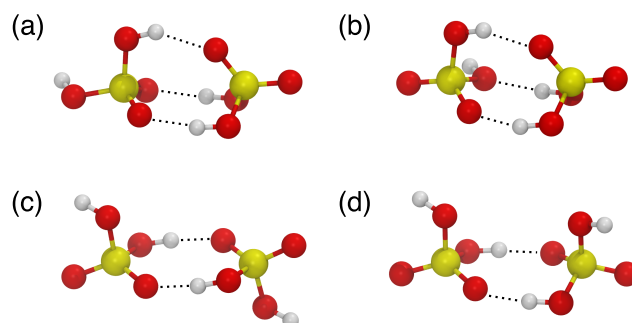


**Figure 1.** Four minimum energy structures for the sulfuric acid dimer (a–d) used to benchmark the force fields by Ding et al. (2003) and Loukonen et al. (2010) against ab initio calculations by Temelso et al. (2012). Sulfur atoms are yellow, oxygens red and hydrogens white. Hydrogen bonds are indicated by dotted lines.

**Table 1.** Relative energies  $\Delta\Delta E$  and hydrogen bond distances  $d_{O\dots H}$  for the sulfuric acid dimer structures (a–d) in Fig. 1 obtained with the force fields by Ding et al. (2003) and Loukonen et al. (2010) and from ab initio calculations by Temelso et al. (2012).

	Structure	a	b	c	d
$\Delta\Delta E$ (eV)	Temelso et al.	0.000	0.032	0.036	0.048
	Ding et al.	0.000	0.081	0.052	0.045
	Loukonen et al.	0.180	0.099	0.004	0.000
$d_{O\dots H}$ (Å)	Temelso et al.	1.92	1.74	1.75	1.75
		1.89	1.91	1.75	1.75
		1.90	1.87		
	Ding et al.	2.00	1.84	1.75	1.74
		1.87	2.31	1.74	1.74
		1.88	1.85		
	Loukonen et al.	1.91	1.84	1.72	1.72
		1.85	1.87	1.72	1.72
		1.83	1.83		

90 from a well-tempered metadynamics simulation (Barducci et al., 2008), using the PLUMED plug-in (Tribello et al., 2014) for LAMMPS (Plimpton, 1995). We used a Velocity Verlet integrator with a time step of 1 fs, to correctly resolve the motion of the hydrogen atoms. The Lennard-Jones interactions were cut off at 14 Å and electrostatic interactions were only evaluated in direct space, with a cut-off at 40 Å. We employed 24 random walkers and Gaussians with a width of 0.1 Å and initial height of  $k_B T$  were deposited every 500 steps along the collective variable and a harmonic wall was used to restrict it to values below

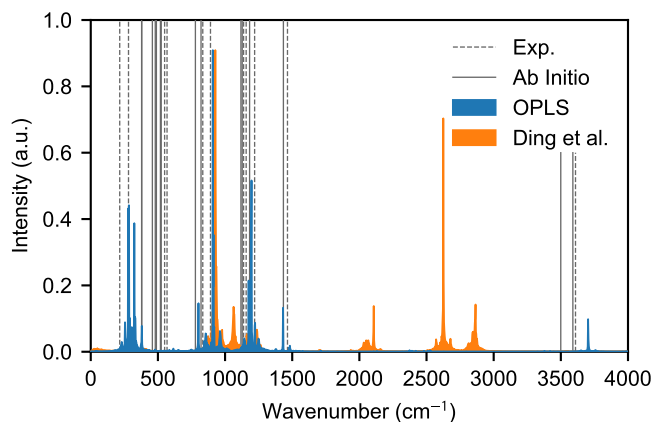


**Figure 2.** Vibrational spectra of the sulfuric acid molecule obtained with OPLS (Loukonen et al., 2010) (blue area) and the force field by Ding et al. (2003) (orange area). The spectra of Ding et al. has its highest frequency mode at  $6565\text{ cm}^{-1}$  outside of the range of the figure. The positions of the peaks in the experimental spectra (Hintze et al., 2003; Chackalackal and Stafford, 1966; Miller et al., 2005) and ab initio calculations (Miller et al., 2005) are indicated by dashed and solid grey lines, respectively.

95  $35\text{ \AA}$ . A bias factor of 5 was chosen, and a Nosé–Hoover chain thermostat of length 5 with a time constant of 0.1 ps was used  
to keep a temperature  $T = 300\text{ K}$ . The combined length of the trajectories was 120 ns for each force field. Both PMFs, shown  
in Fig. 3, exhibit a minimum at  $r = 4.1\text{ \AA}$ , and the binding free energies are  $\Delta F = -0.29\text{ eV}$  and  $-0.27\text{ eV}$  for Loukonen  
et al., and Ding et al., respectively. This is in excellent agreement with the value of  $\Delta G = -0.30\text{ eV}$  obtained from ab initio  
calculations by Temelso et al. (2012) at 298.15 K, and more recent calculations at higher level of theory, which predict slightly  
100 weaker binding ( $-0.23$  to  $-0.26\text{ eV}$ ) (Elm et al., 2016; Mylly et al., 2017).

### 2.3 Collision simulation setup

Molecular dynamics simulations were performed with the LAMMPS code, using a Velocity Verlet integrator with a time step  
of 1 fs. The Lennard-Jones interactions were cut off at  $14\text{ \AA}$  and electrostatic interactions were only evaluated in direct space,  
with a cut-off at  $120\text{ \AA}$ . The simulations were carried out in the NVE ensemble, as the colliding molecules constitute a closed  
105 system (in atmospheric conditions collisions with the carrier gas are rare on the time scale of collisions between sulfuric  
acid molecules). In order to determine the molecules' collision probability as a function of impact parameter and relative  
velocity, the following setup was used: first, two sulfuric acid molecules were placed in the simulation box, separated by  
 $100\text{ \AA}$  along x and the impact parameter  $b$  was set along the z direction, ranging from 0 to  $17.5\text{ \AA}$  in steps of  $0.5\text{ \AA}$ . Atomic  
velocities were randomly assigned from a Maxwell–Boltzmann distribution at  $T = 300\text{ K}$ , and the centre of mass motion of  
110 each molecule removed separately. Then the system was evolved for 50 ps, to randomise the intermolecular orientation and  
ensure equipartition of energy along the intramolecular degrees of freedom. At  $t = 50\text{ ps}$ , each molecule received a translational  
velocity along the x direction,  $v_x = \pm v/2$ , where  $v$  denotes the relative velocity, to set them on a potential collision course. The

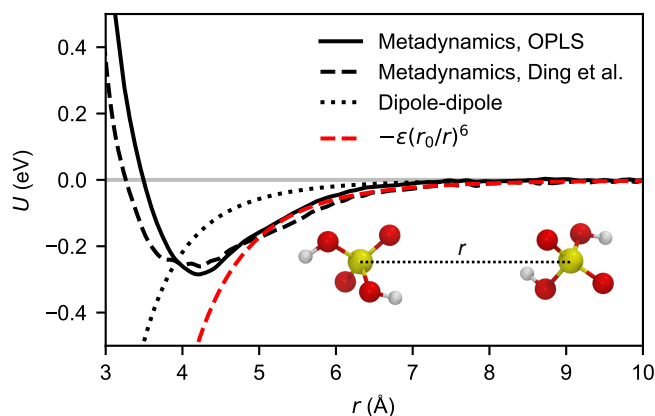


**Figure 3.** Potential of mean force between two  $\text{H}_2\text{SO}_4$  molecules as a function of the sulfur–sulfur distance calculated by metadynamics simulation for the OPLS force field (Loukonen et al., 2010) (solid black line) and the force field by Ding et al. (2003) (dashed black line). For comparison, the Keesom (thermally averaged permanent dipole–permanent dipole) interaction between two point dipoles of 3.07 Debye at 300 K is depicted by the dotted line. The dashed red line shows the attractive potential (Eq. (5)) fitted to the tail of the calculated PMF curve of the OPLS force field.

simulation was continued for another 250 ps, to ensure the possibility of a collision, even at the smallest relative velocities. For a collision of two identical molecules with molecular mass  $m$ , the relative velocities follow the Maxwell–Boltzmann distribution with reduced mass  $\mu = m/2$ . We sampled relative velocities between 50 and 800  $\text{ms}^{-1}$ , in steps of 50  $\text{ms}^{-1}$ . 99 % of the distribution lies within this range at  $T = 300$  K. For each value of the impact parameter  $b$  and the relative velocity  $v$ , 1000 simulations were carried out starting with different initial atomistic velocities, to ensure good sampling. Sulfuric acid molecules bind to each other through the formation of one or more hydrogen bonds. However, even if a collision course leads to an attachment of the two molecules, a portion of the kinetic energy will be redistributed on the degrees of freedom of the formed complex, and this excess energy can lead to a rapid dissociation in the absence of a thermalizing medium. To automate the analysis of over half a million individual trajectories, we define a collision as a trajectory during which the electrostatic energy ( $E_{\text{Coul}}$ ) is lower than a threshold value of  $-0.25$  eV in at least 10 consequent frames (100 ps), indicative of the formation of one or more hydrogen bonds. Three examples of simulated trajectories with relative velocity closest to the mean velocity at 300 K ( $350 \text{ ms}^{-1}$ ) and impact parameter of  $8.5 \text{ \AA}$  are illustrated in Fig. 4.

The results from the atomistic simulations will be compared to different theoretical models described in the following.

## 2.4 Classical model of capture in a field of force

The interaction between two identical polar molecules is usually written as

$$V = \frac{(\mathbf{d}_1 \cdot \mathbf{d}_2) - 3(\mathbf{d}_1 \cdot \mathbf{n})(\mathbf{d}_2 \cdot \mathbf{n})}{r^3} + U(r), \quad (2)$$

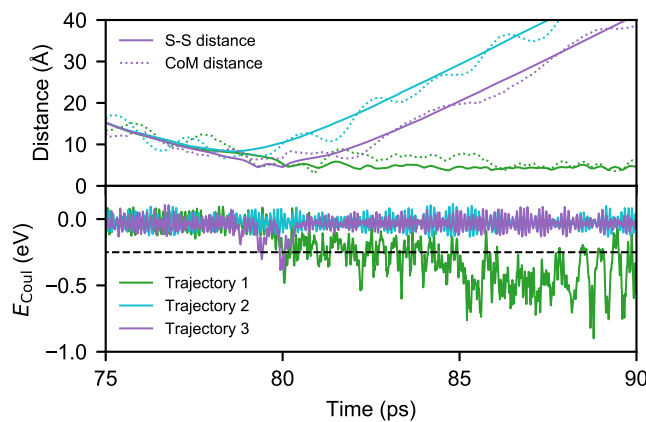


**Figure 4.** Three example MD trajectories with relative velocity of  $350 \text{ ms}^{-1}$  and impact parameter of  $8.5 \text{ \AA}$  after 50 ps of energy relaxation and first 25 ps of collision simulation. The upper panel shows both the distance between the two sulfur atoms (solid lines) and the centre-of-mass distance of the molecules (dotted lines) during the simulations. The electrostatic energies  $E_{\text{Coul}}$ , which is used to determine the possible collision event, for successful (1), unsuccessful (2) and successful but instantly evaporating (3, continuously 0.18 ps below the threshold) trajectories are shown in the lower panel with the threshold value (dashed black line).

where  $d_1$  and  $d_2$  are the dipole moment vectors of the molecules,  $n$  is the unit vector along the distance vector  $r$  connecting the centres of mass of the molecules, and  $U(r)$  is a spherically symmetric potential, usually proportional to  $r^{-6}$ . The capture rate constant for such a potential can only be calculated numerically (Maergoiz et al., 1996c). In the present section we consider only the isotropic part  $U(r)$  of the interaction described by Eq. (2), the effect of anisotropic part (first term in Eq. (2)) is discussed in Appendix A. Then, the Langevin model of capture (Langevin, 1905) can be used to calculate the critical impact parameter beyond which point-like colliding particles in vacuum will escape from each other. Here, the motion of the two colliding molecules is reduced to a one-body problem in an external central field by using an effective potential containing dispersion and centrifugal terms (Landau and Lifshitz, 1976),

$$U_{\text{eff}}(r) = U(r) + \frac{L^2}{2\mu r^2}, \quad (3)$$

where  $r$  is the distance of the colliding body from the centre of the field,  $L$  the angular momentum. Both the total energy of the system (which equals the initial translational energy  $\mu v^2/2$  at  $r \rightarrow \infty$ ) and the angular momentum are conserved. The centrifugal term introduces an energy barrier, and for a successful capture at the barrier ( $r = r_{\text{max}}$ ) the translational energy  $\mu v_{\text{max}}^2/2$  has to be positive. Since the angular momentum equals  $L = \mu v b$ , the condition for  $b^2$  to ensure a capture is

$$b^2 < r_{\text{max}}^2 \left( 1 - \frac{2U(r_{\text{max}})}{\mu v^2} \right). \quad (4)$$

In case of a simple attractive potential (repulsive forces can be neglected, as the studied velocities are relatively low),

$$U(r) = -\epsilon \left( \frac{r_0}{r} \right)^6, \quad (5)$$



145 the square of the critical impact parameter can be written as

$$b_c^2 = \left( \frac{27\epsilon}{2\mu v^2} \right)^{1/3} r_0^2. \quad (6)$$

It is preferable to consider the squared value of  $b$ , since the capture cross section is calculated as  $\sigma_c = \pi b_c^2$ . It is important to note that in the Langevin model, the total energy is divided strictly to the translational and potential energy, the internal degrees of freedom of the two bodies are considered to be completely decoupled, i.e. exchange of translational energy to rotations and vibrations that will occur in a real molecule is completely neglected.

To compare the Langevin model to atomistic simulation results using the OPLS force field, we fitted a potential described by Eq. (5) to the attractive part of the PMF from metadynamics, shown in Fig. 3, and obtained the parameters  $\epsilon = 0.57$  eV and  $r_0 = 4.1$  Å.

## 2.5 Brownian model of aerosol coagulation

155 In the study by Kürten et al. (2014), a model of Brownian coagulation in a field of force (Sceats, 1986, 1989) was used to estimate the collision enhancement factor for neutral cluster formation involving sulfuric acid in a free molecule regime (Chan and Mozurkewich, 2001). The model is based on solving the Fokker–Planck equation for a pair of Brownian particles whose motion is determined by a thermal random force (Sceats, 1986). In the paper by Chan and Mozurkewich (2001), the Hamaker constant describing the strength of the van der Waals interaction was fitted to experiments with uncharged  $\text{H}_2\text{SO}_4/\text{H}_2\text{O}$  particles with diameters of 49–127 nm, yielding a collisions enhancement factor value of 2.3 at 300 K. Although the Hamaker constant is usually considered to be size-independent, there may be enhanced interaction for very small particle sizes, with radii of the order of 1 nm (Pinchuk, 2012).

For the attractive potential described by Eq. (5), the collision enhancement factor over the kinetic gas theory rate,  $W_B = \beta_B/\beta_{\text{HS}}$ , from the Brownian coagulation model in the free molecule limit can be written as (Sceats, 1989)

$$165 \quad W_B = \left( \frac{3\epsilon}{k_B T} \right)^{1/3} \left( \frac{r_0}{2R} \right)^2 \exp\left(\frac{1}{3}\right), \quad (7)$$

where  $\epsilon$  and  $r_0$  are the fitted potential parameters.

## 3 Results and Discussion

The statistics of the collision probabilities as a function of the square of the impact parameter,  $P(b^2)$ , obtained from the atomistic simulations are shown in Fig. 5. The shapes of the simulated curves are sigmoidal and the collision probability is close to unity as  $b$  approaches zero. However, the collision probability decreases slightly at high relative velocities where rapid re-dissociation of the complex can be caused by high kinetic energy and slow redistribution of the energy to vibrational modes of the formed cluster. At the slowest velocity of  $50 \text{ ms}^{-1}$ , and small values of the impact parameter, the collision probability is also reduced. This happens because in some cases the fluctuations in the intermolecular energy, just as they come within



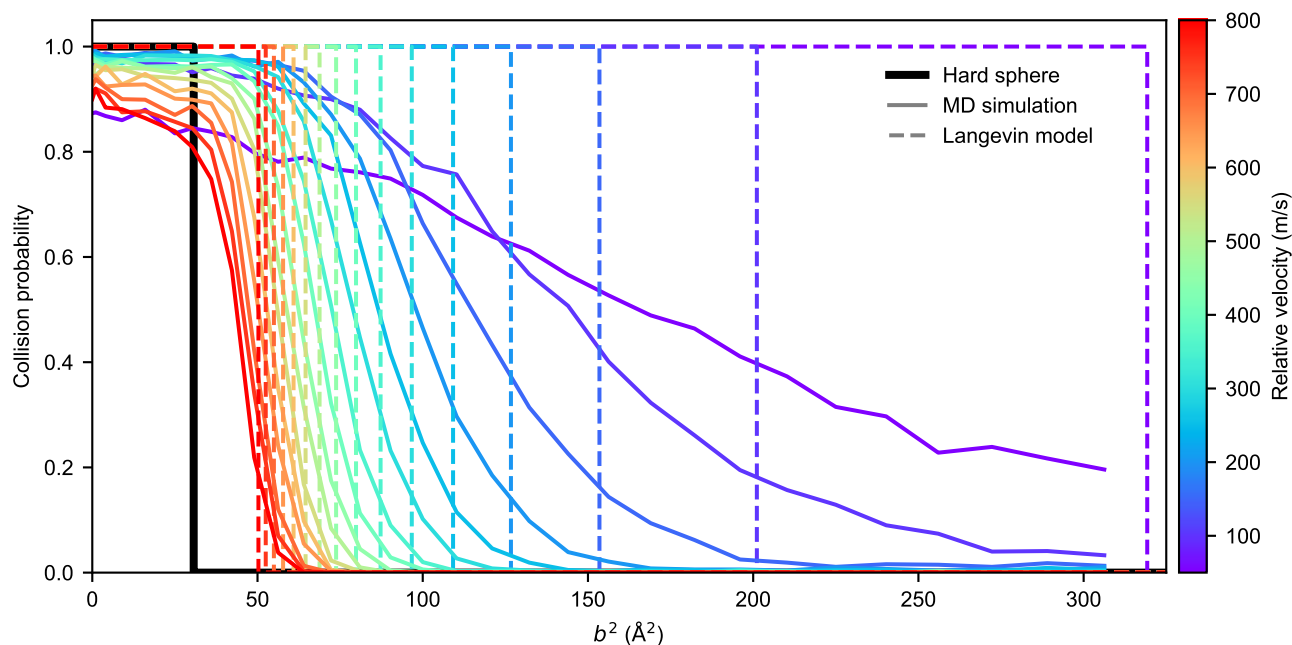


**Figure 5.** Collision probabilities of sulfuric acid molecules, as a function of the impact parameter squared, for different values of the relative velocity, obtained from molecular dynamics simulation (solid coloured lines). The step-like collision probabilities for a hard-sphere model ( $b^2 = (2R)^2$ ), or obtained from the Langevin capture model (Eq. (6)), are indicated by the solid black, and dashed coloured lines, respectively.

interaction range, are sufficient to exceed the very small initial translational energies of the colliding molecules, effectively repelling them (see Appendix B for more detailed discussion).

The dynamical collision cross section, obtained from the integral over the collision probability functions,

$$\sigma_d = \pi \int_0^{\infty} db^2 P(b^2), \quad (8)$$

is consistently decreasing with relative velocity  $v$ . Even though it can be clearly seen in Fig. 5 that values of  $\sigma_d$  are smaller than the corresponding Langevin capture cross sections  $\sigma_c$ , the velocity dependence of the change in  $\sigma_d$  is in very close agreement with the Langevin model solution

$$\frac{\sigma_c(v)}{\sigma_c(v_0)} = \left( \frac{v}{v_0} \right)^{-2/3}, \quad (9)$$

where  $v_0$  is a reference velocity, as shown in Fig. 6. The importance of contributions from long-ranged interactions to the collision cross section is evident, as  $\sigma_c$  is proportional to  $v^{-4/n}$ , for interactions decaying with  $r^{-n}$ . Furthermore, as can be seen in Fig. 5, the critical impact parameters from the Langevin model are matching rather well with the tails of the simulated collision probability curves, the intersection is located without exception at  $P(b^2) \approx 0.2$ .

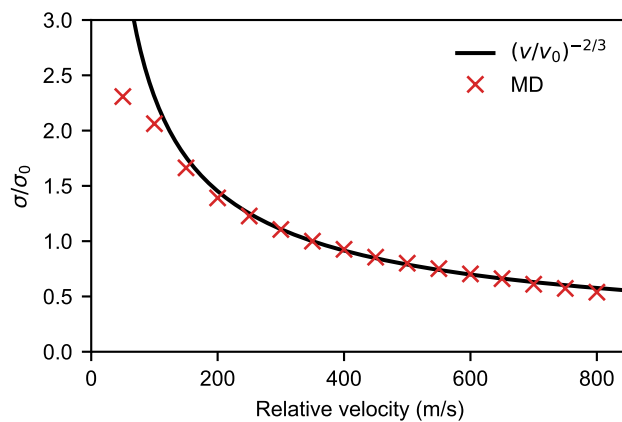


**Figure 6.** Ratio between collision cross section  $\sigma$  and a reference value  $\sigma_0$  as a function of relative velocity. Here the reference value  $\sigma_0$  is the cross section corresponding to relative velocity  $v_0 = 350 \text{ ms}^{-1}$ . The red crosses show the ratio of dynamical cross sections obtained from MD simulations, and the solid black line shows the relation predicted by the Langevin model in Eq. (9).

The discrepancy between  $\sigma_d$  and  $\sigma_c$  is the result of the assumptions made in the Langevin model, where the capture is considered to be orientation-independent and the particles do not have any internal structure. If the anisotropy of the dipole–dipole potential is taken into account, as in Eq. (2), the capture cross section will be reduced (this has been estimated in Appendix A using a numerical approach provided by Maergoiz et al. (1996c)). However, if two molecules are able to move rather close  
190 to each other, translational energy can be transferred to rotational and vibrational modes, and therefore the motion over the centrifugal barrier is hindered, and the critical impact parameter effectively reduced. Additionally, steric hindrance caused by intermolecular orientations incompatible with the formation of hydrogen bonds will also lower the collision probability. Due to coupling, steric hindrance and other dynamical effects, the ratio between the cross sections  $\sigma_d$  and  $\sigma_c$  is on average 0.82 for the collision of two sulfuric acid molecules.

195 The canonical collision rate coefficient can be calculated similarly as Eq. (1), but since the collision probabilities  $P(b^2)$  obtained from the atomistic simulations depend on both the velocity and the impact parameter, the MD based collision rate coefficient is calculated by integrating over both the relative velocity distribution  $f(v)$  and  $b^2$  as

$$\beta_{\text{MD}} = \pi \int_0^{\infty} dv \int_0^{\infty} db^2 v f(v) P(b^2). \quad (10)$$

In case of the Langevin model (Eq. (6)) the expression for the canonical capture rate coefficient can be simplified to

$$200 \quad \beta_{\text{L}} = \pi \int_0^{\infty} dv v f(v) b_c^2(v). \quad (11)$$

Instead of absolute values of the coefficients obtained by different approaches, we focus on the enhancement factor  $W$  relative to the kinetic gas theory rate expressed in Eq. (1), where a hard-sphere radius  $R = 2.76 \text{ \AA}$  was calculated from the



bulk liquid density of sulfuric acid,  $\rho = 1830 \text{ kgm}^{-3}$ , assuming a volume fraction of one. Therefore, after performing the integration, the enhancement factor obtained using the Langevin model can be expressed analytically as

$$205 \quad W_L = \frac{\beta_L}{\beta_{HS}} = \frac{\pi}{\sqrt{3}\Gamma(\frac{1}{3})} \left( \frac{16\epsilon}{k_B T} \right)^{1/3} \left( \frac{r_0}{2R} \right)^2, \quad (12)$$

where  $\Gamma(x)$  denotes the Gamma function, and  $\epsilon$  and  $r_0$  are the parameters from the fit to the attractive part of the potential of mean force between two sulfuric acid molecules in vacuum, using the functional form in Eq. (5). The enhancement factor from the Brownian model of aerosol coagulation,  $W_B$ , was calculated analytically from Eq. (7).

We find that  $W_{MD} \approx 2.2$ ,  $W_L \approx 2.64$ , and  $W_B \approx 3.11$  at 300 K. The enhancement factor obtained by atomistic simulations  
210 is in very good agreement with the kinetic modelling on recent experimental results of formation of atmospheric sulfuric acid dimers (Kürten et al., 2014) and small clusters of sulfuric acid, dimethylamine and water (Lehtipalo et al., 2016; Kürten et al., 2018). In these studies, the enhancement factor was estimated to be 2.3–2.7 using the Brownian coagulation model and Van der Waals interactions fitted to experiment, as mentioned earlier, whereas according to our molecular model of long-range interaction the basic Brownian model using a fit to the attractive part of the potential of mean force overestimates the rate  
215 enhancement factor by over 40 %.

#### 4 Conclusions

In summary, we have benchmarked two classical force fields against experimental and ab initio data and determined that the OPLS force field by Loukonen et al. was able to describe the geometry and vibrational spectra of the isolated sulfuric acid molecule, as well as the geometry and binding free energy of the sulfuric acid dimer. We studied the statistics of collisions  
220 of sulfuric acid molecules in vacuum by molecular dynamics simulations and compared our results against simple theoretical models. We have found that the effective collision cross section of two  $\text{H}_2\text{SO}_4$  molecules, as described by the OPLS force field, is significantly larger than the hard-sphere diameter assigned to the molecule based on the liquid density of sulfuric acid. As a consequence, we find the collision coefficient for sulfuric acid molecules is enhanced by a factor 2.2, compared to kinetic gas theory at 300 K. This enhancement factor obtained from atomistic simulation is consistent with the discrepancy observed  
225 between experimental formation rates of clusters containing sulfuric acid and rates calculated using hard sphere kinetics. The velocity dependence of the dynamical collision cross section is in good agreement with the Langevin model solution. We also note that the enhancement factor obtained from the Langevin model using a fit to the attractive part of the intermolecular potential is within 20 % of the result from the atomistic simulation, at a fraction of the computational cost. In the future, the atomistic collision modelling approach presented in this work can be applied to other atmospherically relevant molecules,  
230 clusters, or ions, exhibiting dipoles of varying magnitude – and in some cases several times larger than the one of the sulfuric acid molecule – to help understand the effect of long-range interactions in cluster formation rates.



## Appendix A: Effect of anisotropy on the dipole–dipole capture rate

Maergoiz et al. (1996c), using classical trajectory integration, calculated the capture rate constant when two identical polar molecules interact through a potential containing anisotropic ( $\propto r^{-3}$ ) and isotropic ( $\propto r^{-6}$ ) terms,

$$235 \quad V = \frac{(\mathbf{d}_1 \cdot \mathbf{d}_2) - 3(\mathbf{d}_1 \cdot \mathbf{n})(\mathbf{d}_2 \cdot \mathbf{n})}{r^3} - \frac{C}{r^6}, \quad (\text{A1})$$

where  $\mathbf{d}_1$  and  $\mathbf{d}_2$  are the dipole moments vectors of the molecules,  $\mathbf{n}$  is the unit vector along the distance vector  $\mathbf{r}$  connecting the centres of mass of the molecules and  $C$  is the isotropic interaction constant.

As in Eq. (1), the capture rate coefficient in an anisotropic field is given by

$$\beta_{\text{aniso}} = \sqrt{\frac{8k_B T}{\pi \mu}} \bar{\sigma}_{\text{aniso}}, \quad (\text{A2})$$

240 where the thermal capture cross section can be calculated using a fitting function  $\kappa(\theta, M)$  as

$$\bar{\sigma}_{\text{aniso}} = \pi \left( \frac{d^2}{k_B T} \right)^{2/3} \theta^{1/6} \kappa(\theta, M), \quad (\text{A3})$$

where  $d$  is the molecular dipole moment (for the OPLS model of sulfuric acid,  $d = |\mathbf{d}_1| = |\mathbf{d}_2| = 3.07$  Debye). Maergoiz et al. use two dimensionless parameters in their model:

$$\theta = \frac{C k_B T}{d^4}, \quad (\text{A4})$$

245 and

$$M = \frac{\mu d^{4/3}}{2I(k_B T)^{2/3}}. \quad (\text{A5})$$

Based on our MD simulations using the OPLS force field, the average moment of inertia  $I$  of a vibrating sulfuric acid molecule is  $100.04 \text{ amu}\text{\AA}^2$ , which deviates slightly from values  $100.66$  and  $104.94 \text{ amu}\text{\AA}^2$  obtained experimentally (Kuczkowski et al., 1981) and from quantum chemical calculations (Zapadinsky et al., 2019), respectively. The fitting function is obtained from  
250 classical trajectory calculations and it is expressed as

$$\ln \kappa(\theta, M) = a_0 + \left( \frac{a_1^2 z}{\sinh(z)} + \frac{z^2}{36} \right)^{1/2}, \quad (\text{A6})$$

where

$$z = a_2 + \ln \theta. \quad (\text{A7})$$

The reported fitting parameters are (Maergoiz et al., 1996c)

$$255 \quad a_0 = 0.2406 - 0.1596 (1 + 1.9192 M^{0.9935})^{-1}, \quad (\text{A8a})$$

$$a_1 = 0.253 - 0.04573 (1 + 1.1645 M^{0.6422})^{-1}, \quad (\text{A8b})$$

$$a_2 = 1.7617 + 0.9577 (1 + 1.9192 M^{0.9935})^{-1}. \quad (\text{A8c})$$

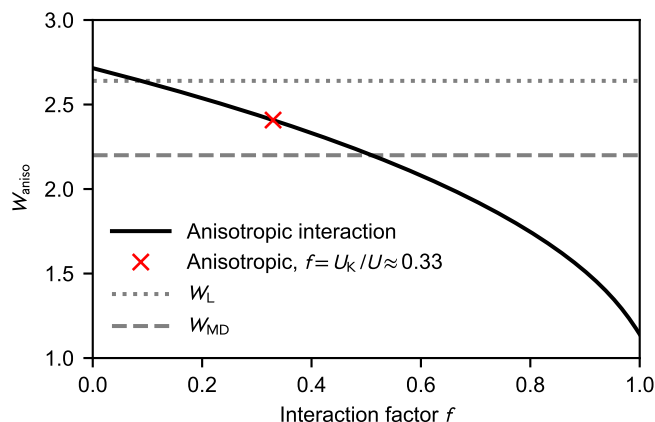


**Figure A1.** Enhancement factor  $W_{\text{aniso}}$  over the kinetic gas theory calculated from the anisotropic dipole–dipole collision cross section as a function of the interaction factor  $f$  at 300 K (black solid line). The red cross denotes the case where the dipole–dipole contribution of the total interaction equals the Keesom equation Eq. (A11) ( $W_{\text{aniso}} = 2.41$ ). The enhancement factors obtained from the Langevin model and the MD simulations are shown as the dotted and dashed grey lines, respectively.

Since all different long-range interactions are included in the attractive part of the potential of mean force between two sulfuric acid molecules (Eq. (5)), to exclude the dipole–dipole interaction from the isotropic interaction, the constant  $C$  is written as

$$C = (1 - f)\epsilon r_0^6, \quad (\text{A9})$$

where  $f$  is a factor denoting the relative magnitude of the anisotropic interaction between permanent dipoles with respect to the total interaction, and  $\epsilon = 0.57$  eV and  $r_0 = 4.1$  Å. Thus, the rate coefficient is controlled by the relative dipole–dipole interaction and the enhancement factor over the kinetic gas theory can be written as

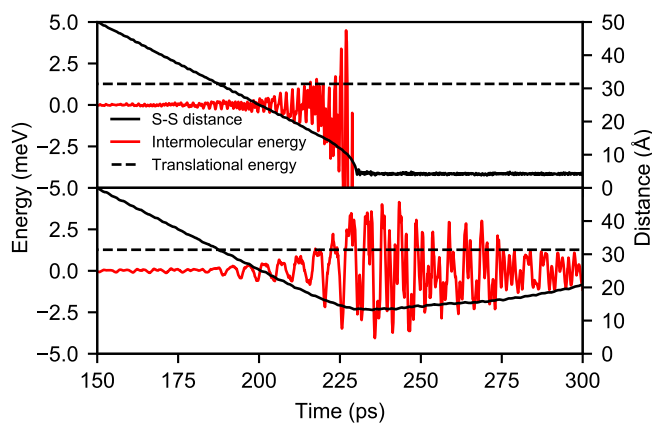
$$W_{\text{aniso}}(f) = \frac{\beta_{\text{aniso}}(f)}{\beta_{\text{HS}}} = \frac{\bar{\sigma}_{\text{aniso}}(f)}{\pi(2R)^2}. \quad (\text{A10})$$

Figure A shows the rate enhancement as a function of the interaction factor  $f$  at 300 K. As the anisotropic part does not contribute, i.e.  $f = 0$ , the enhancement factor is only 3 % higher than the value obtained from the Langevin model (the statistical error of the thermal capture cross section is about 2 % (Maergoiz et al., 1996c)).

Since we are unable to distinguish the actual dipole–dipole interaction from the total attractive potential, we have estimated the interaction using the Keesom equation (see Fig. 3):

$$U_{\text{K}} = \frac{2d^4}{3k_{\text{B}}Tr^6}. \quad (\text{A11})$$

According to Eqs. (5) and (A11), about one third of the attractive potential is due to dipole–dipole interaction at 300 K, and consequently the enhancement factor is  $W_{\text{aniso}} = 2.41$ . Thus, by taking into account the anisotropy of the intermolecular



**Figure B1.** Time evolution of the intermolecular energy (red line) and the sulfur–sulfur distance (solid black line) in one MD trajectory with relative velocity  $v = 50 \text{ ms}^{-1}$  and  $b = 0 \text{ \AA}$  where a collision occurs (top) and one where the molecules are repelled at range (bottom). The initial translational kinetic energy of the molecules (1.27 meV) is indicated by the dashed black line.

potential, the estimated capture rate is in better agreement with the result obtained using atomistic simulation ( $W_{\text{MD}} \approx 2.2$ )  
275 than with the isotropic Langevin model ( $W_{\text{L}} \approx 2.64$ ) as illustrated in Fig. A1.

## Appendix B: Intermolecular repulsion at low velocities in MD simulations

As shown in Fig. 5, for small values of the impact parameter and initial relative velocity between two colliding molecules in the atomistic simulations, the collision probability can be considerably smaller than unity, which seems counter-intuitive at first. This is due to the fact that the intermolecular interaction is anisotropic and the molecules are rotating, which can  
280 lead to instantaneous repulsion even at distances where the intermolecular potential of mean force is slightly attractive. If the initial translational kinetic energy is low enough, the temporary fluctuations in intermolecular energy can alter the translational motion and eventually lead to a definitive separation of the molecules.

This process is illustrated in Fig. B1, which shows the evolution of the intermolecular energy and distance in one trajectory with  $b = 0 \text{ \AA}$  and  $v = 50 \text{ ms}^{-1}$  where a collision occurs and a second one where the molecules are repelled at range. While  
285 in both cases the fluctuation of the intermolecular energy exceeds the initial translational energy of 1.27 meV, in the trajectory exhibiting a repulsion, the large positive energy fluctuations are longer lived and dominate the interaction.

*Author contributions.* RH and BR planned the simulation setup and performed benchmark calculations. BR carried out collision and meta-dynamics simulations and wrote the first draft of the paper. RH and EZ provided the theoretical framework. RH analyzed the simulation data. TK and HV helped plan the project and all authors contributed to writing the manuscript.



290 *Competing interests.* The authors declare that they have no conflict of interest.

*Acknowledgements.* This work was supported by the European Research Council (project 692891 DAMOCLES), Academy of Finland (Academy Research Fellow project 1266388 and ARKTIKO project 285067 ICINA), and University of Helsinki, Faculty of Science AT-MATH project. Computational resources were provided by CSC–IT Center for Science, Ltd., Finland.



## References

- 295 Almeida, J., Schobesberger, S., Kürten, A., Ortega, I. K., Kupiainen-Määttä, O., Praplan, A. P., Adamov, A., Amorim, A., Bianchi, F., Breitenlechner, M., et al.: Molecular understanding of sulphuric acid–amine particle nucleation in the atmosphere, *Nature*, 502, 359, 2013.
- Barducci, A., Bussi, G., and Parrinello, M.: Well-Tempered Metadynamics: A Smoothly Converging and Tunable Free-Energy Method, *Phys. Rev. Lett.*, 100, 020603, 2008.
- 300 Chackalackal, S. M. and Stafford, F. E.: Infrared Spectra of the Vapors above Sulfuric and Deuteriosulfuric Acids, *J. Am. Chem. Soc.*, 88, 723–728, 1966.
- Chan, T. W. and Mozurkewich, M.: Measurement of the coagulation rate constant for sulfuric acid particles as a function of particle size using tandem differential mobility analysis, *J. Aerosol Sci.*, 32, 321–339, 2001.
- Chesnavich, W. J., Su, T., and Bowers, M. T.: Collisions in a noncentral field: a variational and trajectory investigation of ion–dipole capture, 305 *J. Chem. Phys.*, 72, 2641–2655, 1980.
- Clary, D.: Calculations of rate constants for ion-molecule reactions using a combined capture and centrifugal sudden approximation, *Mol. Phys.*, 54, 605–618, 1985.
- Ding, C. G., Taskila, T., Laasonen, K., and Laaksonen, A.: Reliable potential for small sulfuric acid-water clusters, *Chem. Phys.*, 287, 7–19, 2003.
- 310 Dugan Jr., J. V. and Magee, J. L.: Capture collisions between ions and polar molecules, *J. Chem. Phys.*, 47, 3103–3112, 1967.
- Elm, J., Jen, C. N., Kurtén, T., and Vehkamäki, H.: Strong Hydrogen Bonded Molecular Interactions between Atmospheric Diamines and Sulfuric Acid, *J. Phys. Chem. A*, 120, 3693–3700, 2016.
- Hintze, P. E., Kjaergaard, H. G., Vaida, V., and Burkholder, J. B.: Vibrational and electronic spectroscopy of sulfuric acid vapor, *J. Phys. Chem. A*, 107, 1112–1118, 2003.
- 315 Israelachvili, J. N.: *Intermolecular and Surfaces Forces*, Academic Press, 3rd edn., 2011.
- Jorgensen, W. L., Maxwell, D. S., and Tirado-Rives, J.: Development and Testing of the OPLS All-Atom Force Field on Conformational Energetics and Properties of Organic Liquids, *J. Am. Chem. Soc.*, 118, 11225–11236, 1996.
- Kuczkowski, R. L., Suenram, R. D., and Lovas, F. J.: Microwave spectrum, structure, and dipole moment of sulfuric acid, *J. Am. Chem. Soc.*, 103, 2561–2566, 1981.
- 320 Kürten, A., Jokinen, T., Simon, M., Sipilä, M., Sarnela, N., Junninen, H., Adamov, A., Almeida, J., Amorim, A., Bianchi, F., et al.: Neutral molecular cluster formation of sulfuric acid–dimethylamine observed in real time under atmospheric conditions, *Proc. Natl. Acad. Sci. USA*, 111, 15019–15024, 2014.
- Kürten, A., Li, C., Bianchi, F., Curtius, J., Dias, A., Donahue, N. M., Duplissy, J., Flagan, R. C., Hakala, J., Jokinen, T., Kirkby, J., Kulmala, M., Laaksonen, A., Lehtipalo, K., Makhmutov, V., Onnela, A., Rissanen, M. P., Simon, M., Sipilä, M., Stozhkov, Y., Tröstl, J., Ye, 325 P., and McMurry, P. H.: New particle formation in the sulfuric acid–dimethylamine–water system: reevaluation of CLOUD chamber measurements and comparison to an aerosol nucleation and growth model, *Atmos. Chem. Phys.*, 18, 845–863, 2018.
- Landau, L. D. and Lifshitz, E. M.: *Mechanics*, vol. 1, *Course of Theoretical Physics*, Butterworth-Heinemann, 3rd edn., 1976.
- Langevin, P.: A fundamental formula of kinetic theory, *Ann. Chim. Phys.*, 5, 245–288, 1905.
- Lehtipalo, K., Rondo, L., Kontkanen, J., Schobesberger, S., Jokinen, T., Sarnela, N., Kürten, A., Ehrhart, S., Franchin, A., Nieminen, T., 330 et al.: The effect of acid–base clustering and ions on the growth of atmospheric nano-particles, *Nat. Commun.*, 7, 11594, 2016.





- Loukonen, V., Kurtén, T., Ortega, I. K., Vehkamäki, H., Pádua, A. A. H., Sellegri, K., and Kulmala, M.: Enhancing effect of dimethylamine in sulfuric acid nucleation in the presence of water – a computational study, *Atmos. Chem. Phys.*, 10, 4961–4974, 2010.
- Loukonen, V., Bork, N., and Vehkamäki, H.: From collisions to clusters: first steps of sulphuric acid nanocluster formation dynamics, *Mol. Phys.*, 112, 1979–1986, 2014.
- 335 Maergoiz, A., Nikitin, E., Troe, J., and Ushakov, V.: Classical trajectory and adiabatic channel study of the transition from adiabatic to sudden capture dynamics. I. Ion–dipole capture, *J. Chem. Phys.*, 105, 6263–6269, 1996a.
- Maergoiz, A., Nikitin, E., Troe, J., and Ushakov, V.: Classical trajectory and adiabatic channel study of the transition from adiabatic to sudden capture dynamics. II. Ion–quadrupole capture, *J. Chem. Phys.*, 105, 6270–6276, 1996b.
- Maergoiz, A., Nikitin, E., Troe, J., and Ushakov, V.: Classical trajectory and adiabatic channel study of the transition from adiabatic to sudden capture dynamics. III. Dipole–dipole capture, *J. Chem. Phys.*, 105, 6277–6284, 1996c.
- 340 Marlow, W. H.: Derivation of aerosol collision rates for singular attractive contact potentials, *J. Chem. Phys.*, 73, 6284–6287, 1980.
- Miller, Y., Chaban, G., and Gerber, R.: Ab Initio Vibrational Calculations for  $\text{H}_2\text{SO}_4$  and  $\text{H}_2\text{SO}_4 \cdot \text{H}_2\text{O}$ : Spectroscopy and the Nature of the Anharmonic Couplings, *J. Phys. Chem. A*, 109, 6565–6574, 2005.
- Moran, T. F. and Hamill, W. H.: Cross Sections of Ion—Permanent-Dipole Reactions by Mass Spectrometry, *J. Chem. Phys.*, 39, 1413–1422, 1963.
- 345 Myllys, N., Olenius, T., Kurtén, T., Vehkamäki, H., Riipinen, I., and Elm, J.: Effect of Bisulfate, Ammonia, and Ammonium on the Clustering of Organic Acids and Sulfuric Acid, *J. Phys. Chem. A*, 121, 4812–4824, 2017.
- Napari, I., Vehkamäki, H., and Laasonen, K.: Molecular dynamic simulations of atom–cluster collision processes, *J. Chem. Phys.*, 120, 165–169, 2004.
- 350 Pinchuk, A. O.: Size-dependent Hamaker constant for silver nanoparticles, *J. Phys. Chem. C*, 116, 20 099–20 102, 2012.
- Plimpton, S.: Fast Parallel Algorithms for Short-Range Molecular Dynamics, *J. Comp. Phys.*, 117, 1–19, 1995.
- Sceats, M. G.: Brownian coagulation in a field of force, *J. Chem. Phys.*, 84, 5206–5208, 1986.
- Sceats, M. G.: Brownian coagulation in aerosols—the role of long range forces, *J. Colloid Interface Sci.*, 129, 105–112, 1989.
- Sedo, G., Schultz, J., and Leopold, K. R.: Electric dipole moment of sulfuric acid from Fourier transform microwave spectroscopy, *J. Mol. Spectrosc.*, 251, 4–8, 2008.
- 355 Su, T. and Bowers, M. T.: Theory of ion–polar molecule collisions. Comparison with experimental charge transfer reactions of rare gas ions to geometric isomers of difluorobenzene and dichloroethylene, *J. Chem. Phys.*, 58, 3027–3037, 1973.
- Su, T. and Chesnavich, W. J.: Parametrization of the ion–polar molecule collision rate constant by trajectory calculations, *J. Chem. Phys.*, 76, 5183–5185, 1982.
- 360 Su, T., Su, E. C., and Bowers, M. T.: Ion–polar molecule collisions. Conservation of angular momentum in the average dipole orientation theory. The AADO theory, *J. Chem. Phys.*, 69, 2243–2250, 1978.
- Temelso, B., Phan, T. N., and Shields, G. C.: Computational Study of the Hydration of Sulfuric Acid Dimers: Implications for Acid Dissociation and Aerosol Formation, *J. Phys. Chem. A*, 116, 9745–9758, 2012.
- Tribello, G. A., Bonomi, M., Branduardi, D., Camilloni, C., and Bussi, G.: Plumed 2: New feathers for an old bird, *Comput. Phys. Commun.*, 185, 604–613, 2014.
- 365 Troe, J.: Statistical adiabatic channel model for ion–molecule capture processes, *J. Chem. Phys.*, 87, 2773–2780, 1987.
- Zapadinsky, E., Passananti, M., Myllys, N., Kurtén, T., and Vehkamäki, H.: Modeling on Fragmentation of Clusters inside a Mass Spectrometer, *J. Phys. Chem. A*, 123, 611–624, 2019.